Nanoscale Radiative Heat Flow due to Surface Plasmons in Graphene and Doped Silicon

P. J. van Zwol, S. Thiele, C. Berger, W. A. de Heer, and J. Chevrier

Phys. Rev. Lett. **109**, 264301 — Published 27 December 2012

DOI: 10.1103/PhysRevLett.109.264301

Experimental observation of nanoscale radiative heat flow due to surface plasmons in graphene and doped silicon

P.J. van Zwol[1*], S. Thiele[1], C. Berger[1,2], W. A. de Heer[2], J. Chevrier[1*]

1 Institut Néel, CNRS and Universite Joseph Fourier Grenoble, BP 166 38042 Grenoble Cedex 9, France
2 School of Physics, Georgia Institute of Technology, Atlanta, GA 30332, USA.

Owing to its two dimensional electronic structure, graphene exhibits many unique properties. One of them is a wave vector and temperature dependent plasmon in the infrared range. Theory predicts that due to these plasmons, graphene can be used as a universal material to enhance nanoscale radiative heat exchange for any dielectric substrate. Here we report on radiative heat transfer experiments between SiC and a SiO_2 sphere which have non matching phonon polariton frequencies, and thus only weakly exchange heat in near field. We observed that the heat flux contribution of graphene epitaxially grown on SiC dominates at short distances. The influence of plasmons on radiative heat transfer is further supported with measurements for doped silicon. These results highlight graphene's strong potential in photonic nearfield and energy conversion devices.
**Corresponding authors; petervanzwol@gmail.com, joel.chevrier@grenoble.cnrs.fr*

As described by Plancks law, farfield (FF) radiative heat transfer (RHT) is a broadband phenomenon. In contrast in near field (NF) [1-21] surface excitations such as phonon polaritons and low frequency plasmons result in an improved spatial coherence [16] and narrow bandwidths [8], leading to an increase in energy density beyond the Planck blackbody limit [1-3]. For materials such as SiC and SiO_2 the surface excitations are attributed to ion-vibrations [4,5], whereas for doped silicon [11] and graphene [10, 21] they are due to electronic vibrations (plasmons). For these materials, the plasmon frequency can be tuned by changing the amount of free carriers. In addition for graphene the plasmon frequency ω_p is tunable by gating, as it depends on the Fermi level [22-24] furthermore the frequency is wave number (q) and temperature dependent [10]. Thus for a given Fermi level one can find a q for which, in the mid IR, there is a plasmon frequency in graphene that matches that of an excitation in another material (fig. 1a). As a result theory predicts that NF RHT is always enhanced when one or both of the dielectric surfaces are covered with graphene [10].

New opportunities in NF have recently emerged for thermo photo voltaics (TPV) [17-20]. It was previously suggested that in NF, surface excitations can enhance the performance of TPV devices beyond the blackbody limit such that larger efficiencies are reached at lower operation temperatures. The almost monochromatic behavior of NF RHT could yield higher energy conversion efficiencies when properly matched to the bandgap of the PV diodes [17-20]. For example, the frequency of plasmons depends on the carrier density, and can therefore be changed by doping, in materials such as silicon. Optimization of TPV efficiency in NF however is difficult due to proximity effects [20]. Thus the RHT enhancing behavior of graphene [21-26] may play an important role there [21]. While previous experiments reported RHT enhancements due to phonon polaritons [4-6], to date no experiments have reported the effect of plasmons or ultra thin films on NF RHT, this is the aim of the present work.

Our experimental setup is a high vacuum interferometric atomic force microscope (AFM) [5]. A bilayer lever that is sensitive to heat flux [4] acts as probe above a plate that is heated with a Peltier element [14]. The schematics of the AFM and the calibration procedure of the bilayer probe have been reported in ref. [14] in NF and FF. The probe used here is the same as characterized in ref [14]. By fitting RHT measurements for a glass sphere and plate with theory, we calibrated the lever sensitivity $S_h=0.037\pm0.008nW/nm$ and the point of contact due to roughness $d_0=66\pm9nm$. In this study we used the following plates: two 205nm silicon on 400nm insulator samples (SoI 205/400, carrier densities $\sim10^{15}$ (SoI15) and $\sim10^{20}cm^{-3}$ (SoI20)), a bare SiC [000$\bar{1}$] sample and two epitaxial graphene on SiC (EG) [000$\bar{1}$] surfaces with 1-2 (EG2) and 5-6 (EG6) graphene layers. Raman spectra at different places on the surface (Witec 632nm) revealed the typical graphene G- and 2D peaks [24] at 1588±7 and 2660±20cm^{-1} respectively, for both EG samples (fig. 1b) (See [24] for Raman spectra where the SiC contribution is subtracted). The thickness of the EG films was estimated with ellipsometry at 15 places on the surface to be $0.5\pm0.05nm$ for EG2 and $1.5\pm0.2nm$ for EG6. Surface roughness was probed with AFM. Our bare SiC sample shows 0.8nm rms roughness with up to 30nm high peaks.

Graphene layers and pleats (of 20nm high) were typically present on EG surfaces (fig. 1d). For our measurements both SiC and the EG samples were put together on the Peltier ensuring equal experimental conditions. The same was done for the two SoI samples.

Our bilayer lever, while it is rotated 90 degrees [14], is also sensitive to an uncontrolled (probably elec-

trostatic) force. Note that it is not only unique to our setup [4,14]. Whatever the origin of the force, we found that it can be well characterized and subsequently removed from the RHT signal [14]. For the samples used here, this signal was small when compared to the measured RHT [14] but

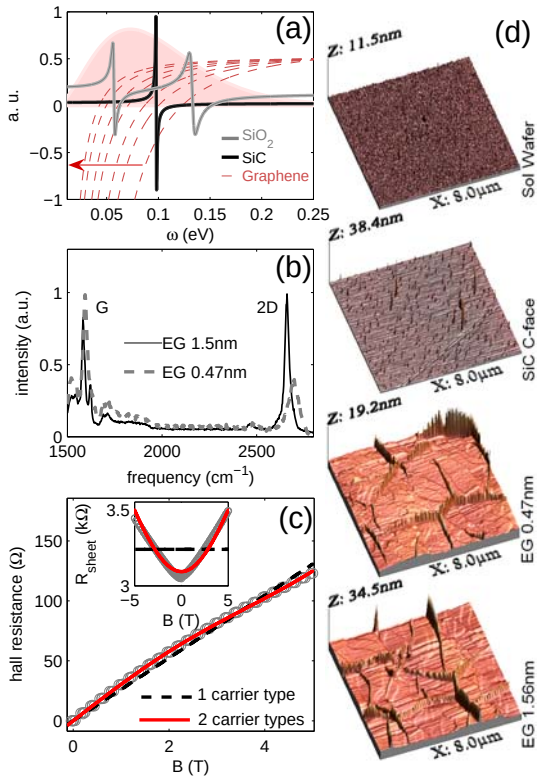

Figure 1; (a) Dielectric functions of SiO_2 and SiC scaled to arbitrary values to compare phonon polariton frequencies to Plancks law at 300K (shaded area) and the q-dependent dielectric function of graphene. The latter is for q in the interval [2.5-20]·10^4 cm^{-1} (arrow), n_h=5·$10^{12}cm^{-2}$ and the relaxation frequency is 10^{13} rad/s [10]. (b) Raman spectra for both EG samples. (c) Hall measurements and theory (fits for 1 or 2 carrier types) [25] for the EG2 sample. Sheet resistance is shown in the inset. (d) AFM scans of the samples in this study.

not negligible. A correction is applied to the measured data at ΔT>0 by subtracting the measured ΔT=0K data. In the supplemental material [28] we show independent measurements and additional analysis of the force measured at ΔT=0 and 40K, that support our claim that it does not change with temperature. We also found no evidence of large temporal or spatial variations of this force. Furthermore we averaged measurements done at multiple spots on the sample. We measured at 7 different locations for both SoI samples, and at 15 different locations for SiC and EG.

The efficiency of NF RHT for silicon and graphene to other materials strongly depends on the plasmon frequency [10,11,21], which in turn depends on the amount of free carriers. For the samples used here the carrier density n_h and mobilities μ were determined by Hall measurements (fig. 1c) in a van der Pauw configuration, with 3mm distance between the contacts, at 4K and 300K using a cryogenic setup and magnetic field up to 5T. For the SoI20 plate the Hall data agreed well for a single type of carriers (holes) with n_h=3.6·$10^{20}cm^{-3}$ and μ=27$cm^2/(V{\cdot}s)$. We estimated n_h=1.06·$10^{15}cm^{-3}$ for the SoI15 sample from resistivity measurements, as far as RHT is concerned SoI15 behaves as intrinsic silicon. The non linear Hall resistance as a function of magnetic field measured in graphene, and significant magneto resistance (fig. 1c) suggest that our EG samples have multiple types of carriers (contribution from the several layers). One could use the classical conductivity tensor method like in [25] to estimate an average n_h and μ of these carriers in each of the graphene layers. However there are multiple solutions to these equations. A simple 2-carrier systems describe the Hall data well, with values in line with the literature for EG2 and EG6 for n_h~1.5-4·$10^{12}cm^{-2}$ and μ~800$cm^2/(V{\cdot}s)$. We stress that the Hall bar of 3mm is fairly large and that the result integrate inhomogeneities, defects, and spatial variation in n_h, μ and the number of EG layers, which complicates this analysis, and makes it unsuitable for use in calculations that are compared to local RHT measurements on microscale areas. It is generally accepted that most carriers in EG are n-type and reside in the layer closest to SiC with n_h=2-4·$10^{12}cm^{-2}$ and μ=1000-10000$cm^2/(V{\cdot}s)$ [23-26]. Inner layers have very low carrier densities (n_h<·$10^{10}cm^{-2}$). The top layer is likely to be almost undoped as well because our setup operates in high vacuum and T_{sample} can reach 375K [27]. Since layers with low carrier density barely contribute to the RHT, we can treat our EG samples as a single conducting layer. Therefore to analyze our RHT data, we will use the present Hall results for doped silicon, and rely on the literature data on micron size Hall bars for EG.

We used standard stochastic electrodynamics [1] to calculate RHT between the two bodies and subsequently used the Derjaguin approximation to obtain results for our plate-sphere system [29]. It is known that this approximation predicts RHT well in NF [14], but underestimates RHT in FF [14,15]. In the case of the SoI15 and SoI20 samples we used multilayer reflection coefficients in the RHT theory. For the SoI20 sample, the carrier scattering time was derived from μ. Together with n_h this defines the Drude term for doped silicon [11]. SiC was optically modeled as a single oscillator [8], and optical data for graphite, silica and sodalime glasses were used from refs. [30-33]. The RHT theory for graphene is based on [10], in which values for n_h and μ from the literature are used.

In our plane-sphere case the FF RHT was much larger than the NF RHT increase with distance (compare

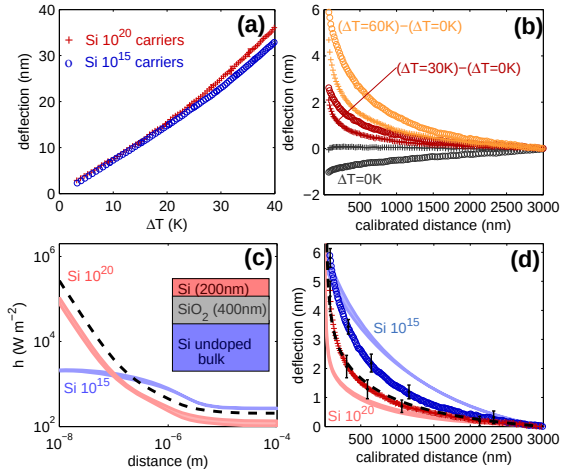

Figure 2: (a) Measurements of FF RHT for both SoI samples. (b) NF RHT measurements for both SoI samples (see legend symbols 2a). Lever deflection is shown for each ΔT. For curves with ΔT>0 the ΔT=0 curve is subtracted. (c) Plane-plane RHT theory in which the Hall results are used, between SiO_2 and both SoI samples. For the latter the multilayer structure is shown. The dashed line represents the optimal Drude parameters for which NF RHT theory matches best the experimental results. (d) Measured average and standard deviation due to spatial variation of NF RHT at 60K as compared to theory (legend in fig. 2c for theory and fig. 2a for experiment applies).

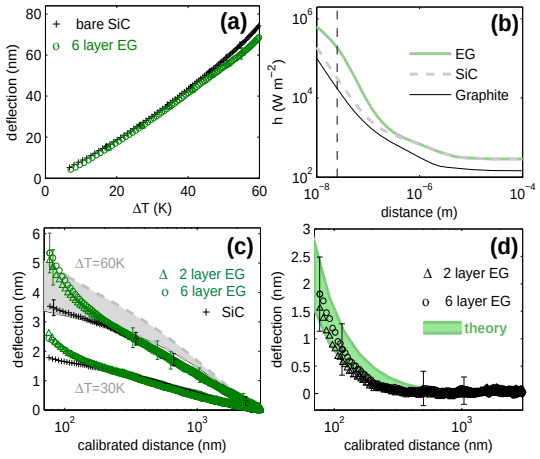

Figure 3: (a) Measured FF RHT. (b) Plane-plane theory between SiO2 and SiC, bulk graphite or EG (single layer $n_h=2\cdot10^{12}cm^{-2}$, $\mu=5000$ $cm^2/(V\cdot s)$) with plate temperatures 300 and 360K. Theory [10] is valid above 25nm (vertical dashed line). (c) Average and standard deviation due to spatial variations, of NF RHT measurements. Theory (grey area) for SiC-silica is also shown in the plane-sphere case. (d) Experimental and theoretical difference in NF RHT between EG-glass and SiC-Glass for ΔT=60K. Here the optical properties of glass matter less in the theory.

fig. 2a and 2d). For this reason experiment was compared to theory separately for the NF and FF regimes. For all the measurements below, we used the calibration values, d_0 and S_h as obtained by fitting RHT theory to experiment for the glass-glass measurements reported earlier [14]. The NF RHT-distance curves were shifted vertically so that at 3μm the values are zero for both theory and experiment, and the FF contribution is effectively subtracted from the NF curves. Then the measurements were shifted horizontally to d_0 and theory was scaled with S_h.

Figure 2 depicts measurements and theory for RHT measured between the SiO_2 sphere and the SoI plates. In FF we found that RHT was almost the same for the two SoI samples (fig. 2a). The measured FF RHT was 25% lower for SiO_2-Silicon than for SiO_2-SiO_2 (see ref. 14), in good agreement with theory. In NF our measurements (fig. 2b) indicate a reduced RHT from plate to sphere for the doped SoI20 sample as compared to the SoI15 sample. We found that RHT increased more rapidly with decreased distance for the SoI20 sample, which is indeed due to the surface plasmon as predicted by theory (fig. 2c). In the plane sphere case RHT is integrated over the sphere area and therefore varying distances. For the present sphere the distance regime around 1μm has a dominant effect. At 1μm, between parallel plates, RHT is larger for the SoI15 sample (fig. 2c). Nonetheless theory and experiment are in reasonable agreement and for both samples and the general behavior is well reproduced (fig. 2d).

Uncertainty in the theory is depicted by plotting the RHT results as an area instead of a line. For the SoI15 sample we used different dielectric data for silica [31-33]. For the SoI20 sample we varied n_h by a factor two around the measured value from *1.8 to 7.2* $10^{20}cm^{-3}$ with corresponding scattering times of *15.5-3.7fsec* as obtained from μ [11]. The optimal parameters for the SoI20 sample were $n_h=1.3\cdot10^{20}cm^{-3}$ with a relaxation time of *10fsec* (fig. 2c,d), which is close to the Hall results. With these values, there is an excellent agreement between theory and measurement in NF (dashed line fig. 2d), and calculated FF underestimates experiment by 20% (figs. 2a,c). Apart from experimental errors in the Hall and RHT measurements additional uncertainty in the calculated curve may come from the use of tabulated optical properties for the 400nm buried oxide (which was modeled as bulk silica). Note that FF RHT is also much more affected by the oxide multilayer structure. Calculations indicated that the effect of the multilayer structure (this thin film effect as compared to bulk Si is not shown in fig. 2c) yielded a 15% increase in FF RHT for the SoI20 sample and a 15% decrease for the SoI15 sample as compared to bulk silicon, while the RHT increase in NF was hardly affected. For doped silicon we could obtain very good agreement with theory by slightly varying n_h around the measured values. But for intrinsic silicon there were no parameters in the theory that could be varied. We suspect that the Derjaguin approximation may be less accurate here because the NF RHT is barely distant dependent in this case (fig. 2c, [28]).

Results for EG are shown in figure 3. In FF we found that graphene had almost no effect on the RHT (fig.

3a). In NF it was clear from each individual measurement curve that, graphene enhanced the RHT significantly below 200nm (fig. 3c,d). This means that the RHT has increased considerably for the area of the sphere closest to the graphene surface (fig. 3b). Note that, on the contrary, RHT would have decreased for bulk graphite (fig. 3b). Furthermore we found no measurable difference in NF RHT between the EG2 and EG6 samples as seen in fig. 3c,d. This result is in agreement with a single layer analysis, and the assumption that the doped graphene layer at the interface dominates.

The calculated NF RHT for SiO_2-SiC in a plate-plate configuration was found to vary by a factor of 5 for different sets of dielectric data for SiO_2 [28, 31-33]. In the plate-sphere case for SiO_2-SiC the calculations varied significantly but only within 20%. For calculations based on the dielectric data of sodalime glass [32,33] the results were 20% higher than the experimental result. The precise result strongly depended on the absorption of silica in the range of the phonon-polariton peak in SiC. Additional uncertainty may come from the use of an oscillator model for SiC.

By taking the difference between the experimental curves with and without graphene, we extracted the effect of graphene on the NF RHT. In fig. 3d, NF RHT calculations for graphene, based on ref. [10] with values for $n_h=[2,4]\cdot10^{12}$ cm^{-2} and $\mu=[1000,10000]$ $cm^2/(V\cdot s)$ as found from the literature, are compared to experiment without any other adjustable parameters. In general we found that the RHT calculations were much more sensitive to n_h than on μ. Also n_h and μ in graphene depend on each other as graphene with lower n_h has higher μ. The effects on RHT calculations offset each other to some extent, and the agreement with RHT experiment remains good for a wide range of n_h and μ values.

Concluding we have experimentally shown that thermally excited plasmons in doped silicon and EG on SiC substantially increase NF RHT. It is intriguing to see that one or a few atomic layers can completely alter NF RHT and that graphene can enhance RHT for materials with non-matching surface excitations. SiC is often used as a cheap emitter in FF TPV devices, and is one of the most promising candidates for large scale graphene fabrication. EG grown on SiC may therefore serve as a base for future plasmonic NF TPV devices with increased efficiency beyond the blackbody limit.

Acknowledgements : We gratefully acknowledge support from the Agence Nationale de la Recherche through the Source-TPV project ANR 2010 BLAN 0928 01, from the National Science Foundation (DMR-0820382), the Air Force Office of Scientific Research and the Partner University Fund. The authors benefited from exchange of ideas within the ESF Research Network CASIMIR. We thank N. Bendiab, L. H. Diez, L. Ranno, F. Gay and J. Marcus for help on Raman and Hall measurements.

References

[1] D. Polder and M. Van Hove, Phys. Rev. B 4, 3303 (1971).
[2] C. M. Hargreaves, Phys. Lett. 30 A, 491 (1969).
[3] A. Kittel, W. Müller-Hirsch, J. Parisi, S. A. Biehs, D. Reddig, M. Holthaus, Phys.Rev. Lett. 95, 224301 (2005).
[4] S. Shen, A. Narayanaswamy, and G. Chen, Nano Lett. 9, 2909 (2009). S.Shen, A. Mavrokefalos, P.Sambegoro, G. Chen, Appl. Phys. Lett. 100, 233114 (2012).
[5] E. Rousseau, A. Siria, G. Jourdan, S. Volz, F. Comin, J. Chevrier, and J-J. Greffet, Nat. Photonics 3, 514 (2009).
[6] R. S. Ottens, V. Quetschke, Stacy Wise, A. A. Alemi, R. Lundock, G. Mueller, D. H. Reitze, D. B. Tanner, and B. F. Whiting, Phys. Rev. Lett. 107, 014301 (2011).
[7] T. Kralik, P. Hanzelka, V. Musilova, A. Srnka, and M. Zobac, Rev. Sci. Instrum. 82, 055106 (2011).
[8] J.-P. Mulet, K. Joulain, R. Carminati, and J.-J. Greffet, Appl. Phys. Lett. 78, 2931 (2001).
[9] I. Volokitin and B. N. J. Persson, Rev. Mod. Phys. 79, 1291 (2007), ibid. Phys. Rev. B 83, 241407(R) (2011).
[10] V. B. Svetovoy, P.J. van Zwol, J. Chevrier, Phys. Rev. B 85, 155418 (2012)
[11] C. J. Fu and Z. M. Zhang, Int. J. Heat Mass Transfer 49, 1703 (2006).
[12] M. Francoeur, M. P. Mengüç, and R. Vaillon, Appl. Phys. Lett. 93, 043109 (2008).
[13] S.-A. Biehs *and* J.-J. Greffet *Phys. Rev. B 82, 245410 (2010).*
[14] P. J. van Zwol, L. Ranno, J. Chevrier, J. Appl. Phys, 111, 063110 (2012), Ibid, Phys. Rev. Lett. 108, 234301 (2012).
[15] C. Otey, S. Fan, Phys. Rev. B 84, 245431 (2011).
[16] J. -J. Greffet, R. Carminati, K. Joulain, J. -P. Mulet, S. Mainguy, and Y. Chenet, Nature (London) 416, 61 (2002).
[17] R. S. DiMatteo, P. Greiff, S. L. Finberg, K. A. Young-Whaite, H. K. H. Choy, M. M. Masaki, and C. G. Fonstad, Appl. Phys. Lett. 79, 1894 (2001).
[18] M. D. Whale and E. G. Cravalho, IEEE Trans. Energy Convers. 17, 130 (2002).
[19] A. Narayanaswamy and G. Chen, Appl. Phys. Lett. 82, 3544 (2003).
[20] M. Laroche, R. Carminati, and J.-J. Greffet, J. Appl. Phys. 100, 063704 (2006).
[21] O. Ilic, M. Jablan, J. D. Joannopoulos, I. Celanovic, and M. Soljačić, Optics Express, 20, A366-A384 (2012).
[22] K. S. Novoselov, A. K. Geim, S. V. Morozov, D. Jiang, Y. Zhang, S. V. Dubonos, I. V. Gregorieva, and A. A. Firsov, Science 306, 666 (2004).
[23] C. Berger et al., Science 312, 1191 (2006).
[24] W. A. de Heer, C. Berger, M. Ruan, M. Sprinkle, X. Li, Y. Hu, B. Zhang, J. Hankinson, and E. Conrad, PNAS 108, 16900 (2011).
[25] Y. Lin et al, Appl. Phys. Lett. 97, 112107 (2010).
[26] J. L. Tedesco, B. L. VanMil, R. L. Myers-Ward, J. M. McCrate, S. A. Kitt, P. M. Campbell, G. G. Jernigan, J. C. Culbertson, J. C. R. Eddy, and D. K. Gaskill, Appl. Phys. Lett. 95, 122102 (2009).
[27] M. Sprinkle, D. Siegel, Y. Hu, J. Hicks, P. Soukiassian, A. Tejeda, A. Taleb-Ibrahimi, P. Le Fèvre, F. Bertran, S. Vizzini, H. Enriquez, S. Chiang, C. Berger, W.A. de Heer, A. Lanzara, E.H. Conrad, Phys. Rev. Lett., 103, 226803 (2009).
[28] See supplemental material…
[29] B. V. Derjaguin, Kolloid-Z. 69, 155 (1934).
[30] H.R. Philipp, Phys. Rev. B 16, 2896 (1977).
[31] R. Kitamura, L. Pilon, and M. Jonasz, Appl. Opt. 46, 8118 (2007).
[32] P. J. van Zwol, G. Palasantzas, and J. Th. M. DeHosson, Phys. Rev. E 79, 041605 (2009).
[33] B.G. Bagley, et al. Crys. Solids. 22 423, (1976)